Available online at www.sciencedirect.com
SCIENCE DIRECT®
Optical Materials 28 (2006) 306–309
OPTICAL Materials
www.elsevier.com/locate/optmat

Thermal stability and spectral properties of Er^{3+}-doped gadolinium borosilicate glasses

Jiangting Sun [a], Jiahua Zhang [a,*], Yongshi Luo [a], Shaozhe Lu [a], Xinguang Ren [a], Baojiu Chen [a], Xiaojun Wang [a,b,*]

[a] *Key Laboratory of Excited State Processes, Changchun Institute of Optics, Fine Mechanics and Physics, Chinese Academy of Sciences, 16 East–South Lake Road, Changchun 130033, PR China*
[b] *Department of Physics, Georgia Southern University, Statesboro, GA 30460, USA*

Received 29 July 2004; accepted 11 January 2005
Available online 24 February 2005

Abstract

A new glass of Gd_2O_3–B_2O_3–SiO_2–Na_2O–Er_2O_3 system is prepared and the formation range of the glass is experimentally obtained. Excellent thermal stability of the glass has been demonstrated using differential thermal analysis. Effects of the B_2O_3 content on the infrared spectral properties such as the 1.5 μm emission bandwidth and the Judd–Ofelt parameter Ω_t ($t = 2, 4, 6$) of Er^{3+} ions in the glass has been observed. The glass exhibits a large integrated emission cross sections for the 1.5 μm emission band. The Er^{3+}-doped gadolinium borosilicate glass is a great candidate for broadband erbium doped fiber amplifiers.

PACS: 42.70.C; 78.20.C; 81.05.Pj

1. Introduction

In recent years, Er^{3+}-doped glasses with a broad 1.5 μm emission band have been extensively investigated in searching erbium-doped fiber amplifiers (EDFA) with a wide and flat gain spectrum that is required for dense wavelength division multiplexing (DWDM) optical network systems in the telecommunication [1–7]. Among the reported Er^{3+}-doped glasses, Er^{3+}-doped tellurite glasses have shown wide 1.5 μm emission bandwidths and a large stimulated emission section. Mori reported excellent performance of a tellurite based EDFA, which gave 80 nm-wide gain around 1.5–1.6 μm [5]. However, tellurite glasses have relatively poor thermal stability in comparison with silicate glasses. Tanabe et al. reported on bismuth-based glasses $43Bi_2O_3$–xB_2O_3–$(57 - x)SiO_2$ with a bandwidth about 75 nm [7], but the description on thermal stability was unknown. In addition, thermal stability of Bi_2O_3–B_2O_3–Na_2O glass reported by Yang [8], in which the glass transition temperature (T_g) and the temperature difference (ΔT) only in excess of 415 and 123 °C, respectively. In this article, we report the preparation and the formation range of glass and the thermal stability of Er^{3+}-doped gadolinium borosilicate glasses, Gd_2O_3–B_2O_3–SiO_2–Na_2O–Er_2O_3 (GBSN:Er). A wide formation range of glass is experimentally obtained. Special attention was paid on $10Gd_2O_3$–$(80 - x)B_2O_3$–$xSiO_2$–$10Na_2O$–$0.5Er_2O_3$ (G_{10}BSN:Er and $x = 0$, 10, 20, 30, and 40 mol%), which shows high thermal stability. Spectral properties of the glass are also characterized. To our knowledge, there have been no research reports published yet concerning this glass system.

* Corresponding authors. Tel./fax: +86 431 617 6317.
E-mail address: zjiahua@public.cc.jl.cn (J. Zhang).

0925-3467/$ - see front matter © 2005 Elsevier B.V. All rights reserved.
doi:10.1016/j.optmat.2005.01.001

2. Experimental

GBSN:Er glasses, in which the content of compositional Na_2O is always 10 mol%, were prepared from anhydrous powders of Gd_2O_3, B_2O_3, SiO_2, Na_2O, and Er_2O_3 with more than 99.9% purity. After melting the powders in a platinum crucible at 1400–1450 °C for 1.5 h, they are poured into pre-heated brass molds. After the formation range of glass was confirmed, the G_{10}BSN:Er glasses were prepared. The quenched samples are annealed around 500 °C for 12 h and then cooled inside the furnace down to room temperature. The obtained G_{10}BSN:Er glasses have been named GS_0, GS_{10}, GS_{20}, GS_{30}, and GS_{40} glasses, corresponding to the SiO_2 content (x) of 0, 10, 20, 30, and 40 mol%, respectively.

Emission spectra were recorded using a TRIAX 550 spectrometer with a spectral resolution of 1 nm under excitation of 980 nm laser diode. Absorption spectra were obtained using a Perkin–Elmer 9 Lambda spectrometer. The differential thermal analysis (DTA) data was collected using a Perkin–Elmer 7 Series Thermal Analysis System.

3. Results

Fig. 1 shows the formation range of the GBSN:Er glass system. The symbols '●', '○', and '△' denote glass, non-glass and half glass state, respectively. The directions of arrowhead show the increase of the host content. The glass phase can be formed only when the content of SiO_2 is 0–50 mol%, Gd_2O_3 is 0–30 mol% and B_2O_3 is above 20 mol% in this glass system. The glass can also be obtained but becomes translucent at the contents of 60 mol% SiO_2 and 30 mol% Gd_2O_3, or at the contents of 60 mol% SiO_2 and 30 mol% B_2O_3. There is no glass phase formed in other glass components. In addition, Na_2O is added into the material for the diminution of the melting temperature of the glass.

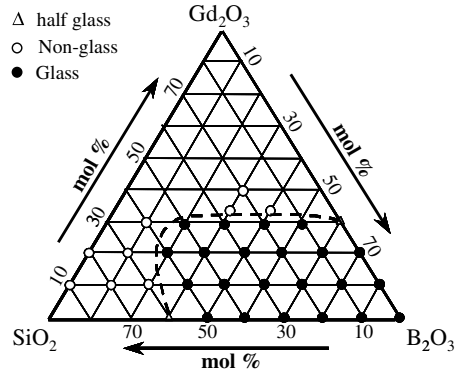

Fig. 1. Formation range of GBSN:Er glass system.

Fig. 2 shows the compositional dependence of glass transition temperature T_g (■), crystallization onset temperature T_x (▲), and the temperature difference $\Delta T = T_x - T_g$ (●) in the G_{10}BSN:Er glasses. It is found that both T_g and T_x increase as the SiO_2 content increases (up to $x = 30$) and the difference ΔT reaches a maximum of 193 °C at $x = 20$. The values of T_g (>590 °C) and ΔT (133–193 °C) in the G_{10}BSN:Er glasses are both higher than the corresponding temperatures in bismuth borate glass ($T_g > 415$ °C; 170 °C > ΔT > 123 °C) [8] and tellurite glass ($T_g > 290$ °C; 130 °C > ΔT > 90 °C) [9]. The G_{10}BSN:Er glass exhibits excellent thermal stability.

The spectral properties of glasses including 1.5 μm bandwidth are directly related to Judd–Ofelt (J–O) parameters, which can be obtained by analyzing absorption spectra. Fig. 3 gives the absorption spectra of the G_{10}BSN:Er glasses recorded at room temperature. The spectra consist of seven absorption bands peaking at 1527, 975, 796, 652, 541, 520 and 488 nm, corresponding to the transitions from the ground state $^4I_{15/2}$ to the

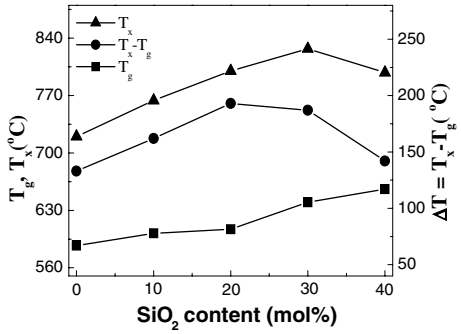

Fig. 2. Compositional dependence of glass transition temperature T_g onset crystallization temperature T_x and the difference $T = T_x - T_g$ in the G_{10}BSN:Er glasses. The SiO_2 content 0, 10, 20, 30, and 40 mol% are responsible to the sample GS_0, GS_{10}, GS_{20}, GS_{30}, and GS_{40}, respectively.

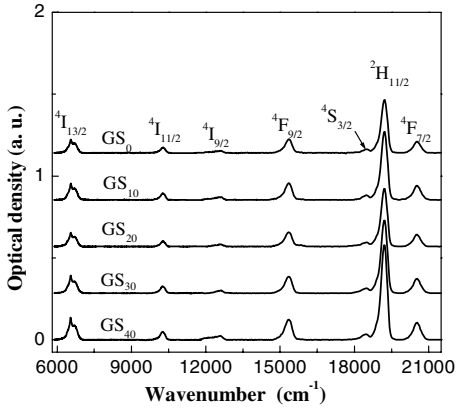

Fig. 3. The absorption spectra of the G_{10}BSN:Er glasses recorded at room temperature.

excited states $^4I_{13/2}$, $^4I_{11/2}$, $^4I_{9/2}$, $^4F_{9/2}$, $^4S_{3/2}$, $^2H_{11/2}$ and $^4F_{7/2}$ of Er^{3+} ion, respectively.

The radiative transition within the $4f^n$ configuration of Er^{3+} can be analyzed by use of the J–O theory [10,11]. The electric dipole transition line strength S_{ed} between two J states can be expressed as [12]

$$S_{ed}(J;J') = \sum_{t=2,4,6} \Omega_t \langle \alpha SL, J \| U^{(t)} \| \alpha' S' L', J' \rangle^2 \quad (1)$$

where Ω_t ($t = 2, 4, 6$) is the Judd–Ofelt parameter, αSL the other quantum numbers of the states, and the $\langle \| U^{(t)} \| \rangle$ the doubly reduced matrix elements of unit tensor operators calculated in the intermediate coupling approximation. The Ω_t parameters can be obtained from a least-squares fit of Eq. (1) to the line strengths of above-mentioned seven absorption bands. J–O parameters are the indicators of the local structure of the Er^{3+}-doped host. The Ω_2 parameter is affected by the covalent chemical bonding and the Ω_4 and Ω_6 parameters are related to the rigidity of the medium where the Er^{3+} ions are situated.

Fig. 4 depicts the relationship between the Ω_t parameters of Er^{3+} and the B_2O_3 content in the G_{10}BSN:Er glasses. It can be seen that Ω_2 decreases with the increase of B_2O_3 content, while Ω_6 increases monotonically. There is a weaker degree of covalency of Er–O bond at the GS_0 glass, because the Ω_2 reaches minimum value at the GS_0 glass. In addition, comparing Ω_4 and Ω_6, the rigidity and viscosity of the GS_{30} glass matrix are larger than that of all other glasses, because both the Ω_4 and Ω_6 reach minimum value at the GS_{30} glass.

Fig. 5 illustrates the emission spectra of the $^4I_{13/2}$ to $^4I_{15/2}$ transition of Er^{3+} ions in the G_{10}BSN:Er glasses, where the area under the emission spectral profile is normalized. Because of the differences of the emission spectra in different glass hosts, the full width at half maximum (FWHM) is often used as a semiquantitative indication of the bandwidth. As shown in Fig. 5, the FWHM of the emission increases from 60 to 70 nm as the content of B_2O_3 increases from 0 to 40 mol%.

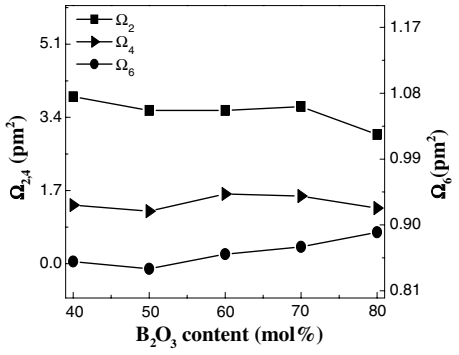

Fig. 4. The relationship between the $\Omega_{t(2,4,6)}$ parameters of Er^{3+} and the B_2O_3 content in the G_{10}BSN:Er glasses. The B_2O_3 content 40, 50, 60, 70, and 80 mol% are responsible to the sample GS_{40}, GS_{30}, GS_{20}, GS_{10}, and GS_0, respectively.

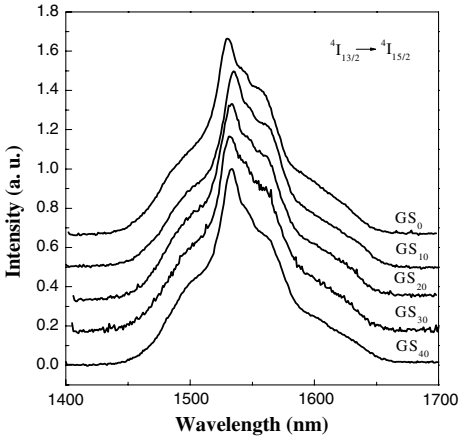

Fig. 5. The normalized 1.5 μm emission spectra of Er^{3+} in the G_{10}BSN:Er glasses with different B_2O_3 compositions.

Table 1
The values of the excitation energy E, the absorption and the calculated emission cross sections of Er^{3+} at the peak place

Sample name	λ_{abp} (nm)	λ_{emp} (nm)	E (cm^{-1})	σ_a^{peak} (10^{-20} cm^2)	σ_e^{peak} (10^{-20} cm^2)
GS_0	1527	1533	6531	0.3318	0.3469
GS_{10}	1527	1533	6556	0.3915	0.4592
GS_{20}	1526	1534	6526	0.3876	0.3994
GS_{30}	1529	1535	6546	0.4475	0.5188
GS_{40}	1528	1535	6551	0.3956	0.4665

The absorption cross section is obtained by using absorption spectra of the sample. According to the theory of McCumber [13], the stimulated emission cross section $\sigma_e(\lambda)$ can be calculated using the following expression:

$$\sigma_e(\lambda) = \sigma_a(\lambda) \exp\left[\left(E - \frac{hc}{\lambda}\right) \Big/ kT\right] \quad (2)$$

where $\sigma_a(\lambda)$ is the absorption cross section of the transition from the $^4I_{15/2}$ state to the $^4I_{13/2}$ state, E the temperature-dependent excitation energy, k the Boltzmann constant and T the temperature of the sample. The values of the excitation energy E, the absorption and the calculated emission cross sections of Er^{3+} ions at the peak place are listed in Table 1. Both the absorption and emission cross sections of Er^{3+} reach a maximum of 0.45×10^{-20} and 0.52×10^{-20} cm^2 at the GS_{30} glass, respectively, as shown in Table 1.

4. Discussion

According to Eq. (1), the S_{ed} of the Er^{3+} ions is expressed as

$$S_{ed}[^4I_{13/2}; {}^4I_{15/2}] = 0.019 \times \Omega_2 + 0.118 \times \Omega_4 + 1.462 \times \Omega_6 \quad (3)$$

Evidently, the Ω_6 plays a dominant role in broadening the bandwidth of the 1.5 μm emission among the three Ω_ts. Thus increasing the Ω_6 parameter will result in the increase of the 1.5 μm emission bandwidth. Hence, both of the Ω_6 and the 1.5 μm emission bandwidth increase with the increase of B_2O_3 content in the G_{10}BSN:Er glasses, as shown in Fig. 6.

The gain bandwidth of optical amplifier can be evaluated by integrated emission cross section, estimated by the product of FWHM $\times$ σ_e^{peak} where σ_e^{peak} is the emission cross section at the peak of 1.5 μm band. The bigger the product is, the better the gain characteristic of EDFA yields. Fig. 7 represents the FWHM $\times$ σ_e^{peak} product of Er^{3+} in different glass hosts. It can be seen that the value of the FWHM $\times$ σ_e^{peak} product in the prepared glasses are more than those of germanate [14], silicate [15] and phosphate [16] glasses. Furthermore, the maximum value of the product among these glasses reported in this work is smaller than that of oxyfluoride silicate glass [17], which have a bigger integrated emission cross section in the previous reported glasses.

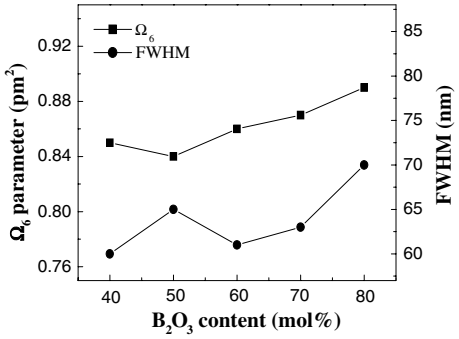

Fig. 6. The dependence of both of the Ω_6 value and the 1.5 μm emission bandwidth on the content of B_2O_3 in the G_{10}BSN:Er glass of Er^{3+} ions. The content of B_2O_3 is 40, 50, 60, 70, and 80 mol% are responsible to the sample GS_{40}, GS_{30}, GS_{20}, GS_{10}, and GS_0, respectively.

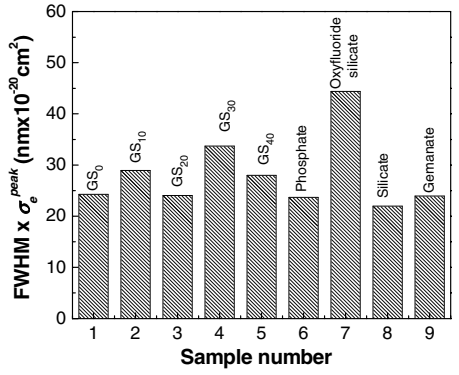

Fig. 7. The FWHM $\times$ σ_e^{peak} product of Er^{3+} in different glass hosts.

5. Conclusions

A new glass of GBSN:Er glasses system is prepared, and formation range of the glass is experimentally obtained. On the analysis of DTA data, the Er^{3+}-doped G_{10}BSN:Er glasses exhibit high thermal stability with glass transition temperatures higher than 590 °C. The glasses exhibit broad 1.5 μm emission band around 70 nm, which are much larger than that of silica glasses with a narrow emission bandwidth around 30 nm presenting use. In addition, the glasses also have larger area of integrated emission cross sections than germanate, silicate and phosphate glasses. Therefore, the Er^{3+}-doped glass GBSN:Er system is a promising host for the EDFA in the 1.5 μm window telecommunication system.

Acknowledgments

The authors acknowledge the supports by the National Natural Foundation of China under grant no. 90201010, the Natural Science Foundation of Jilin Province of China, under grant no. 20030104, and 'One Hundred Talents Project' of Chinese Academy of Sciences.

References

[1] V.K. Tikhomirov, D. Furniss, A.B. Seddon, Appl. Phys. Lett. 81 (11) (2002) 1937.
[2] Q.P. Chen, M. Ferraris, D. Milanese, Y. Menke, E. Monchiero, G. Perrone, J. Non-Cryst. Solids 324 (2003) 12.
[3] S.Q. Man, S.F. Wong, E.Y.B. Pun, J. Opt. Soc. Am. B 19 (8) (2002) 1839.
[4] X. Feng, S. Tanabe, T. Hanada, J. Am. Ceram. Soc. 84 (1) (2001) 165.
[5] A. Mori, Y. Ohishi, S. Sudo, Electron. Lett. 33 (1997) 863.
[6] J.S. Wang, E.M. Vogel, E. Snitzer, Opti. Mater. 3 (1994) 187.
[7] S. Tanabe, N. Sugimoto, S. Ito, T. Hanada, J. Lumin. 87–89 (2000) 670.
[8] J.H. Yang, S.X. Dai, J. Appl. Phys. 93 (2) (2003) 977.
[9] X. Zou, T. Izumitani, J. Non-Cryst. Solids 162 (1993) 68.
[10] B.R. Judd, Phys. Rev. 127 (3) (1962) 750.
[11] G.S. Ofelt, J. Chem. Phys. 37 (3) (1962) 511.
[12] M.J. Weber, J.D. Myers, D.H. Blackbern, J. Appl. Phys. 52 (4) (1981) 2944.
[13] K. Hirano, Y. Benino, T. Komatsu, J. Phys. Chem. Soc. 62 (2001) 2075.
[14] H. Lin, E.Y.B. Pun, S.Q. Man, J. Opt. Soc. Am. B 18 (2001) 602.
[15] X.L. Zou, I. Teturo, J. Non-Cryst. Solids 162 (1993) 68.
[16] S. Jiang, T. Luo, B.C. Hwang, J. Non-Cryst. Solids 263–264 (2000) 364.
[17] S.Q. Xu, Z.M. Yang, S.X. Dai, J. Alloys Comp. 361 (2003) 313.